Properties of dissipative Floquet Majorana modes using a quantum dot

Nicolò Forcellini [1,*] Zhan Cao [1] and Dong E. Liu [2,1,3]

[1] *Beijing Academy of Quantum Information Sciences, Beijing 100193, China*

[2] *State Key Laboratory of Low Dimensional Quantum Physics, Department of Physics, Tsinghua University, Beijing 100084, China*

[3] *Frontier Science Center for Quantum Information, Beijing 100084, China*

(Received 31 January 2023; revised 25 April 2023; accepted 26 April 2023; published 9 May 2023)

We study the electronic conductance of dissipative Floquet Majorana zero modes (FMZMs) in a periodically driven nanowire coupled to a quantum dot. We use a numerical method which can accurately take into account the dissipation effects from the superconducting bath, which causes the FMZMs to have a finite lifetime. Our results show that, in the weak nanowire-dot coupling regime, the peak conductance at zero temperature of the resonant dot can be well approximated by a universal function of the FMZM lifetime rescaled with the nanowire-dot coupling strength. For a long FMZM lifetime, the conductance approaches the characteristic quantized value of $G = e^2/2h$, whereas $G \to e^2/h$ (uncoupled dot) as the FMZMs' lifetime goes to zero. Moreover, we show how the conductance-lifetime relation is modified when considering the full Floquet structure of the nonequilibrium Green's function, undesired coupling to non-Majorana states, a nonresonant quantum dot, and finite-temperature effects. Assuming good control over the system parameters, our method can be used to test the presence and lifetime of FMZMs in such devices, which is key for any practical application of these topological states.

DOI: 10.1103/PhysRevB.107.195412

I. INTRODUCTION

Topological superconductors can host zero-energy modes, also called *Majorana zero modes* (MZMs) [1,2], which, if experimentally engineered, have the potential to make topological quantum computation practical [3,4] due to to their non-Abelian braiding properties [4–7]. MZMs have, so far, proven to be extremely difficult to engineer experimentally. A possible platform is given by semiconductor nanowires with spin-orbit coupling proximitized to an s-wave superconductor (SC) [8–12]. Seeking the realization of Majorana modes in such devices has been the subject of extensive research in the past decade, with recent experimental progress [13–26].

Topological states of matter and nontrivial band structures can also be accessed through Floquet engineering, i.e., the control of quantum systems through the application of a controlled periodic drive [27–48]. The characteristic "replicated" Floquet band structure in energy space for solid-state systems has been experimentally verified through time and angle-resolved photoemission spectroscopy [49–51]. In particular, Floquet methods can induce a topological phase transition, while the static system is topologically trivial, as for the case of Floquet Majorana modes (FMMs), the periodically driven equivalent of MZMs [34,36,37]. The study of nonequilibrium phases of matter that can exhibit FMMs has been an active field of research in the past years, as it connects the field of topology in condensed matter to problems in nonequilibrium physics such as prethermalization, thermalization, and disorder in open/closed quantum systems, time crystals, etc. [52–59]. Specifically, open quantum systems can show a complicated behavior in particle statistics, depending on the details of the bath and the system-bath coupling [60–63]. In addition, recent works about realistic Floquet superconductors [64] and on dissipative FMMs in nanowires [65] highlight the importance of taking the SC bath-nanowire coupling into account. In the presence of dissipation, while bosonic condensation in the SC survives in the presence of a periodic drive, fermionic quasiparticles, including FMMs, acquire a finite lifetime which the standard Floquet theorem cannot correctly capture.

Therefore, in this work we further investigate the lifetime of dissipative Floquet Majorana zero modes (FMZMs) [65]. The effects of dissipation from the superconducting bath are taken into account using the Floquet-Keldysh formalism, which allows us to realistically model the SC bath embedding the system [64–66]. We model a setup which would allow to experimentally probe the lifetime of the dissipative FMZMs, see Fig. 1. The setup consists of a quantum dot (QD) resonantly coupled to a FMZM located at the end of a nanowire, which is periodically driven with frequency Ω; two external leads (L,R) are used to measure the QD electronic conductance. We show that reducing the FMZMs' lifetime by increasing the periodic drive amplitude in the nanowire leads to a transition in the QD single-spin conductance from $G = e^2/2h$ (Majorana mode signature, see, e.g., [67]) to $G = e^2/h$ (resonant uncoupled dot).

In the weak nanowire-dot coupling regime, the conductance in the presence of dissipation in the nanowire-SC system can be modeled by using a finite-lifetime (MZM) toy model, with the conductance being a universal function of the FMZM lifetime rescaled with respect to the nanowire-dot coupling strength. However, the Floquet structure of the FMZMs' Green's function needs to be taken into account for a stronger

*nforcellini@baqis.ac.cn

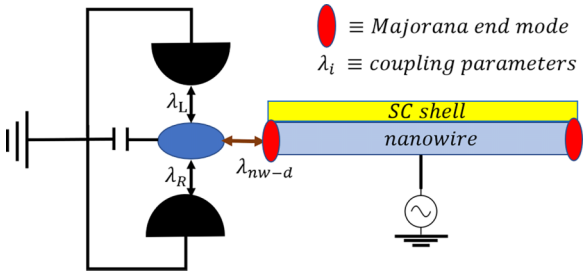

FIG. 1. Setup of the proposed device: The nanowire is periodically driven with frequency Ω, with one of its ends coupled to a quantum dot through an effective coupling λ_{nw-d}. The dot itself is connected to external leads L and R to measure its conductance.

coupling. The functional form of the conductance becomes more complex and deviates from the simpler toy model for short FMZM lifetimes, maintaining the same asymptotic behavior for long lifetimes. Therefore, we show through our results that the QD conductance can be used as a signature of the presence of dissipative FMZMs in periodically driven topological nanowires, and it can also be used as a measure of the FMZM's lifetime in such devices.

The paper is organized as follows: In Sec. II we introduce the model of the driven-dissipative nanowire coupled to a QD and derive the expression of the QD Floquet conductance. In Sec. III we present and discuss our numerical results on the QD spectrum and conductance, as well as introduce a toy model that allows for a good physical understanding of the numerical results. Our results are first presented for the case of a resonant dot at zero temperature, and in Sec. III C we show how deviations affect the peak conductance. Finally, in Sec. IV we report our conclusions.

II. MODEL

A. Superconducting nanowire

Consider a one-dimensional (1D) semiconducting nanowire (SM) in the proximity of an *s*-wave superconducting bath. We introduce a periodic drive in the SM region. The 1D Bogoliubov–de Gennes (BdG) Hamiltonian representing such a system is given by

$$H(t) = H_{nw}(t) + H_{sc} + H_c\,; \tag{1}$$

the SM Hamiltonian, in real space, is [65,68]

$$H_{nw}(t) = \int_0^L dx\, \psi_x^\dagger \Big[\Big(\frac{p_x^2}{2m} - \mu + 2A\cos(\Omega t)\Big)\sigma_0\tau_z - \alpha p_x \sigma_y \tau_z + V_z\sigma_z\tau_z\Big]\psi_x, \tag{2}$$

with spinor representation $\psi_x = (c_{x\uparrow}, c_{x\downarrow}, c_{x\uparrow}^\dagger, c_{x\downarrow}^\dagger)^T$, where $c_{x\uparrow/\downarrow}$ annihilates an up-/down-spin electron at location x on the nanowire of length L; μ is the chemical potential; A and $\Omega = 2\pi/\tau$ are the amplitude and frequency of the periodic drive; V_z is the Zeeman energy; and α is the spin-orbit coupling strength. σ_μ and τ_μ indicate the Pauli matrices in the spin and Nambu spaces, respectively. Note that we assume the nanowire to be uniform, and therefore effects such as the appearance of nontopological edge states such as "quasi-Majorana modes" (QMMs), which can be induced by disorder and other imperfections in the nanowire [68–73], are not considered. The study of QMMs for this setup goes beyond the scope of the present work and shall be left for a follow-up study.

In our system the bulk proximity SC also serves as a thermal bath, which we assume to be much "larger" than the SM nanowire system. Indeed, the density of states (DOS) for the normal metal phase of the SC is much larger than that of the SM nanowire. Therefore the thermal energy generated within the system from the drive will be dissipated into the bulk proximity SC. Hence we ignore any transient effect in the nanowire and we assume that the system has reached the nonequilibrium steady state, meaning that energy transfer/heating influx and outflux between the system and the bath are balanced [28,29,65,66]. This leads to a Green's function (GF) periodic with the period τ of the drive $Q(t,t') = Q(t+\tau, t'+\tau)$, which we define as the nonequilibrium Keldysh GF for our full nanowire-QD-external leads system, after integrating out the SC bath degrees of freedom—see below and the Appendix for more details and definitions.

The Hamiltonian of the SC bath is, in the mean-field BdG form in momentum space, $H_{sc} = \sum_q \phi_q^\dagger(\epsilon_q\tau_z - \Delta\sigma_y\tau_y)\phi_q$, where Δ is the SC gap, and $\phi_q = (a_{q\uparrow}, a_{q\downarrow}, a_{-q\uparrow}^\dagger, a_{-q\downarrow}^\dagger)^T$, where $a_{q\uparrow/\downarrow}$ is the annihilation operator for spin-up/-down electrons of momentum q in the SC bath. The SC-nanowire coupling H_c is modeled as follows: First, the nanowire Hamiltonian is discretized with lattice spacing a becoming

$$H_{nw}(t) = \frac{1}{2}\sum_i \psi_i^\dagger\{(2t_h - \mu + 2A\cos\Omega t)\sigma_0\tau_z + V_z\sigma_z\tau_z\}\psi_i - \Big[\psi_{i+a}^\dagger\Big(t_h\sigma_0 + \frac{\alpha}{2a}\sigma_y\Big)\tau_z\psi_i + \text{H.c.}\Big], \tag{3}$$

where the hopping constant $t_h \equiv \hbar^2/2ma^2$.

Then the Markovian approximation [65], through which correlations in the bath are neglected, allows to couple each site of the chain to independent and identical SC baths $H_{sc,i} = \sum_q \phi_{qi}^\dagger(\epsilon_{qi}\tau_z - \Delta\sigma_y\tau_y)\phi_{qi}$. Hence, the coupling Hamiltonian can be expressed as

$$H_c = \sum_{i,q,\sigma} V(c_{i,\sigma}^\dagger a_{q,\sigma} + a_{q,\sigma}^\dagger c_{i,\sigma}). \tag{4}$$

The SC gap Δ and the nanowire-SC coupling V are taken to be real, positive numbers without loss of generality. Choosing the system-bath hybridization V to be independent of the mode q of the bath allows for a simpler treatment of dissipation and amounts to the definition of an "effective" coupling strength [65]. The external degrees of freedom can then be integrated out as shown in [65] using the Floquet theorem, and the resulting effective Floquet Hamiltonian, which includes the energy-dependent bath self-energy correction $\Sigma_{sc}(\omega)$ and on-site Green's function, are reported in the Appendix. The main point is that a finite SC gap Δ broadens the quasiparticle spectrum, representing dissipation caused by the SC bath via the imaginary part of $\Sigma_{sc}(\omega)$. On the other hand, the nondissipative limit $\Delta \to \infty$ is equivalent to the introduction of a simple induced gap term $\Delta_{ind}\sigma_y\tau_y$ in the nanowire,

with induced order parameter $\Delta_{ind} = \pi\rho_F V^2$, where we set $\pi\rho_F = 1$ as the DOS of the SC bath. See the Appendix and [65] for more details on the dissipation model and the large-Δ, nondissipative limit.

B. Coupling the dot

Consider the undriven QD coupled to one of the ends of the nanowire through some effective hopping λ_{nw-d} [67]:

$$H_d = \sum_\sigma \epsilon_d d_\sigma^\dagger d_\sigma + \lambda_{nw-d}\sum_\sigma (d_\sigma^\dagger c_{L,\sigma} + \text{H.c.}) + \sum_{k,\alpha=L,R,\sigma} \lambda_{\alpha\sigma}(c_{k\alpha\sigma}^\dagger d_\sigma + \text{H.c.}) + V_z^d(d_\uparrow^\dagger d_\uparrow - d_\downarrow^\dagger d_\downarrow). \tag{5}$$

In the above, ϵ_d is the dot level and c_L is the annihilation operator for the last site of the nanowire. The two leads labeled as left (L) and right (R) have Hamiltonian $H_{\text{leads}} = \sum_{k,\alpha=L,R} c_{k\alpha\sigma}^\dagger c_{k\alpha\sigma}$ and couple to the dot with a width $\Gamma_{\alpha\sigma} \equiv 2\pi|\lambda_{\alpha\sigma}|^2\rho_{Fl}$, where the lead DOS $2\pi\rho_{Fl} = 1$ is assumed to be constant. $c_{k\alpha\sigma}(d_\sigma)$ denotes the electron annihilation operator for the leads (QD). V_z^d is the Zeeman splitting for the dot, which might be different from V_z of the nanowire, or, when assuming that the QD and nanowire materials are the same, can be set to have the same value. In any case, we assume that the Zeeman energy is the largest scale in the QD, and therefore we can consider only one spin channel, ignoring any electron-electron interaction in the above Hamiltonian. Moreover, we tune the QD such that the energy of the spin-$\downarrow$ electron $\epsilon_d - V_z^d = 0$, allowing this state to be resonant with the FMZM.

From this model, and following the method described in [65], we use the recursive Floquet-Green's function technique to obtain the relevant components of the dot Green's function used for our calculations—see the Appendix for more details.

In this work we investigate the QD conductance due to its coupling to dissipative FMZMs of finite lifetime τ_{FM}. As mentioned in the previous section, a finite SC gap Δ induces dissipation, i.e., a broadening of the quasiparticle spectrum. Our operational definition of the FMZM lifetime is the inverse of the width $\Gamma_{FM} = \tau_{FM}^{-1}$ obtained by fitting the FMZM peak of the spectrum at the end of the nanowire. With the (time-averaged) DOS of a FMZM at the end of the nanowire,

$$\nu_{FM}(\omega) = -\frac{1}{\pi}\text{ImTr}\{Q_{FM}^R(0,\omega)\}, \tag{6}$$

and the retarded FMZM Floquet Green's function having the form $Q_{FM}^R(0,\omega) = [\omega - \Sigma_{FM}(\omega)]^{-1}$, then one has, in the zero-frequency approximation,

$$\nu_{FM}(\omega) \propto \frac{\Gamma_{FM}}{\omega^2 + \Gamma_{FM}^2}. \tag{7}$$

Hence, we identify the self-energy $\Sigma_{FM}(\omega = 0) = -i\Im[\Sigma_{FM}(\omega = 0)] = i\Gamma_{FM}$ in the FMZM Green's function as purely imaginary, since the peak of $\nu_{FM}(\omega)$ is always at $\omega = 0$ for a FMZM. In addition, increasing the driving amplitude A also leads to an increase in dissipation and a decay in quasiparticle lifetime in the nanowire [65]. Hence, we use A as the tuning parameter for the FMZMs' lifetime control. For a more detailed discussion of the definition of Floquet Majoranas' lifetime, we refer to [65]. For this work the above definition suffices.

C. Quantum dot conductance for a Floquet system

The time-dependent current in the left lead is given by

$$I_L(t) = \frac{ie}{\hbar}\sum_{k\sigma}(\lambda_{kL\sigma}c_{kL\sigma}^\dagger d_\sigma - \lambda_{kL\sigma}^* d_\sigma^\dagger c_{kL\sigma}), \tag{8}$$

with the equivalent definition for the current through R. Details of the derivation of the expression for the current $I(t) = I_L(t) + I_R(t)$ through the QD using Floquet-Keldysh field theory are left to the Appendix. Here we report the final expression for the zero-bias time-averaged conductance ($G = d\langle I\rangle/dV|_{V\to 0}$):

$$G = -\frac{2e^2}{\hbar}\int\frac{d\omega}{2\pi}\frac{\Gamma_L\Gamma_R}{\Gamma_L+\Gamma_R}\text{ImTr}\{Q_{dd}^R(0,\omega)\}\left(-\frac{\partial n_F}{\partial\omega}\right). \tag{9}$$

In the above, $n_F(\omega) = [1 + e^{-\hbar\omega/k_BT}]^{-1}$ is the Fermi-Dirac distribution at temperature T, $\Gamma_{L/R}$ are the leads' coupling widths as defined under Eq. (5), and $Q_{dd}^R(0,\omega)$ is the zeroth Fourier component (time average) of the retarded component of the QD GF, defined as, with $t_{rel} = t - t'$,

$$Q_{dd}(n,\omega) = \frac{1}{\tau}\int_0^\tau dt\int_{-\infty}^\infty dt_{rel}e^{-in\Omega t}e^{-i\omega t_{rel}}Q_{dd}(t,t_{rel}) \tag{10}$$

for $n = 0$, where we made use of the periodicity of the GF [66]. In our system we assume that the driving frequency Ω is higher than the other energy scales, which makes it sufficient to compute the time-averaged conductance and allows for efficient numerical calculations. (We keep the driving amplitude-frequency ratio $\kappa \equiv A/\Omega < 1$ for numerical convergence of the Floquet matrices, which are truncated to some [65,66], see the Appendix for more details.) Equation (9) can be seen as the Floquet generalization of the static QD conductance [67].

As a special case, consider symmetric coupling to the leads $\Gamma_L = \Gamma_R = \Gamma$ leading to the peak conductance (as the temperature $T \to 0$):

$$G_{\text{peak}} = -\frac{e^2}{h}\Gamma\ \text{ImTr}\{Q_{dd}^R(0,\omega\to 0)\}. \tag{11}$$

For our numerical calculations of the conductance, we only select the spin $\downarrow$-electron. From now on, G_{peak} will be referred to as G, and Eq. (11) will be used to produce our numerical results for the time-averaged QD conductance.

III. RESULTS AND DISCUSSION

A. Quantum dot spectral function

As a first step, in Fig. 2 we investigate the single-spin spectral function of the dot $A_\downarrow(\omega) \equiv -\Gamma\Im\{Q_{dd,\downarrow}^R(0,\omega)\}$; for simplicity we will drop the $\downarrow$ label. In Fig. 2(a), in the nondissipative limit, the dot spectrum has the same characteristics of a quantum dot coupled to a (non-Floquet, static) Majorana zero mode with the same setup [67]: The dot spectral function $A(0) = 1/2$ whenever the MZM is coupled to the

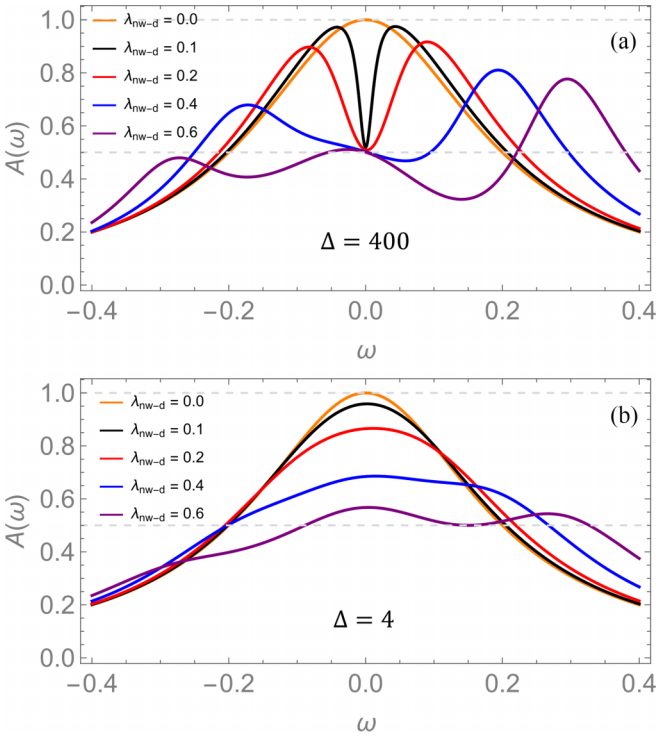

FIG. 2. Quantum dot spectrum when coupled to (a) a nondissipative FMZM, note the value $A(0) = 1/2$, expected from Majorana modes for any $\lambda_{nw-d} \neq 0$, and (b) a dissipative FMZM, with the same parameters as in (a) except for the SC gap Δ. Note how the $1/2$ value at $\omega = 0$ is lost, with $A(0) \to 1$ for small λ_{nw-d}. For the calculations, $\epsilon_d = V_z^d$, placing the $\downarrow$ electron at zero energy. $\Gamma_L = \Gamma_R = \Gamma = 0.1$, $t_h = 2.0$ (bandwidth $D = 4t_h = 8.0$), $\mu = -2.0$, $\alpha = 3.0$, $V_z = V_z^d = 4.0$, $V = 1.2$, $A = 3.0$, and $\Omega = 12.0$.

dot, independently of the coupling strength, and $A(0) = 1$ with $\lambda_{nw-d} = 0$ (resonant isolated dot). This translates in a peak conductance with a value $G = e^2/2h$, which is a signature of MZMs [67]. This is in fact not surprising and can be explained using a simple theoretical argument using standard Floquet theory for time-periodic Hamiltonians [37]. The physical wave function in real space of some Floquet state with quasienergy ϵ is $\Psi(x,t) = e^{i\epsilon t/\hbar}\psi(x,t)$, with $\psi(x,t) = \psi(x,t+\tau)$ satisfying the eigenvalue equation $H_F(x,t)\psi(x,t) = \epsilon\psi(x,t)$, with the Floquet Hamiltonian $H_F(t) = H(x,t) - i\hbar\partial/\partial t$ [74]. Assuming the existence of an $\epsilon = 0$ eigenmode, we can define its wave function $\eta(x,t) \equiv \Psi(x,t) = \psi(x,t)$, defined at any t by the Floquet eigenvalue equation, where t has now assumed the role of a simple parameter. Hence, a MZM exists at each t since $\psi(x,t)$ solves the eigenvalue equation with $\epsilon = 0$. Therefore FMZMs, defined by quasienergy $\epsilon = 0$, are MZMs at all times, i.e., localized at each end of the nanowire, which has also been shown numerically [36,75], leading to the $G = e^2/2h$ signature.

On the other hand, Fig. 2(b) shows the spectrum in the presence of a dissipative FMZM. In this case, the $A(0) = 1/2$ signature is generally lost, with a decreasing λ_{nw-d} leading to $A(0) \to 1$. Intuitively, this is due to the FMZM having acquired a finite lifetime due to dissipation, which approaches the uncoupled limit $A(0) \to 1$ as the lifetime gets shorter

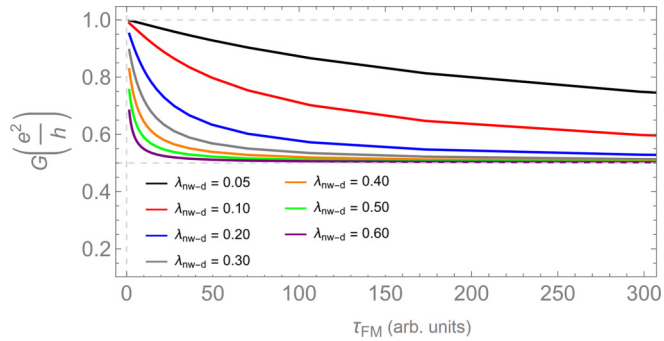

FIG. 3. Conductance G from Eq. (11) as a function of the FMZM lifetime τ_{FM} (arbitrary units), as the nanowire-dot coupling λ_{nw-d} is changed. With a sufficiently long lifetime, the conductance G is stabilized around the topological signature $G = e^2/2h$. A larger value for λ_{nw-d}, meaning a stronger coupling to the finite-lifetime FMZM, leads to a more stable signal around $G = e^2/2h$. Parameters as in Fig. 2 ($\Omega = 12.0$, etc.), with amplitudes $0 \leqslant A \leqslant 5.2$, which allows to tune the lifetime τ_{FM} in the x axis, and $N_F = 10$ the Floquet matrix cutoff.

and/or the coupling λ_{nw-d} gets weaker. λ_{nw-d} should be kept small enough. With the current parameters (see caption of Fig. 2) the induced gap parameter is $\Delta_{ind} = 1.44$, and therefore we must have $\lambda_{nw-d} < \Delta_{ind}$ to limit the undesired influence of modes above the gap. In our calculations, the nanowire has a length $L = 200$ sites, and we set the Floquet cutoff $N_F = 10$ to ensure convergence of the numerics [65]. The parameters used in this work and reported in Figs. 2 and 5 agree with previous works on dissipative and nondissipative FMZMs [37,65], and are consistent with proposals of FMZM realization in cold-atom systems [34].

B. Conductance and FMZMs' lifetime

In order to better understand the conductance signal of the dissipative FMZMs, we show in Fig. 3 the values of G as a function of FMZM lifetime τ_{FM} for different λ_{nw-d}. By increasing the strength A of the Floquet drive (and shortening the FMZM lifetime τ_{FM}) we find a transition between $G = e^2/2h$, indicating the presence of a Floquet Majorana mode, to $G = e^2/h$, which is the conductance of an uncoupled dot resonant at zero energy. A stronger coupling stabilizes the conductance signal around the Majorana signature $G = e^2/2h$. In the following we start from the simplest toy model for dissipative Majorana modes in order to better analyze the numerical results.

1. Toy model of a dissipative Majorana mode

Consider the following toy model for a normal MZM coupled to the dot. The effective Hamiltonian for the single-spin dot-MZM system is

$$H = H_{\text{leads}} + H_T + H_{QD-\text{MZM}}, \tag{12}$$

where [67]

$$H_{QD-\text{MZM}} = \epsilon_d d^\dagger d + \lambda_{nw-d}(d - d^\dagger)\eta_1 + i\delta\eta_1\eta_2, \tag{13}$$

with δ being the exponentially small coupling $\delta \sim e^{-L/\xi}$ with coherence length $\xi = v_F/\Delta_{ind}$, v_F being the Fermi velocity.

Here, we set $\delta = 0$ to isolate one of the Majoranas. H_{leads} and H_T are the single-spin versions of the lead and lead-dot coupling Hamiltonians previously defined after Eq. (5). In order to impose a finite lifetime for η_1, we assign it a width $\Gamma_M(\omega)$ in its GF $Q^R_\eta(\omega) = C_0/[\omega + i\Gamma_M(\omega)]$, where C_0 is a normalization constant.

Assuming symmetric coupling to the leads $\Gamma_L = \Gamma_R = \Gamma$ and $\epsilon_d = 0$, the retarded component $Q^R_{dd}(\omega)$ for this toy model is given by

$$Q^R_{dd}(\omega) = \frac{\left[1 - \frac{C_0|\lambda_{nw-d}|^2}{(\omega+i\Gamma_M(\omega))(\omega+2i\Gamma)}\right]}{(\omega+2i\Gamma)\left[1 - \frac{2C_0|\lambda_{nw-d}|^2}{(\omega+i\Gamma_M(\omega))(\omega+2i\Gamma)}\right]}. \tag{14}$$

This leads to G with the following simple form:

$$G(\tilde{\lambda}) = \frac{e^2}{h}\frac{1 + C_0|\tilde{\lambda}|^2/2\Gamma}{1 + C_0|\tilde{\lambda}|^2/\Gamma}, \tag{15}$$

where $|\tilde{\lambda}|^2 = |\lambda_{nw-d}|^2/\Gamma_M(\omega \to 0) \sim |\lambda_{nw-d}|^2\tau_M$. Hence, we found that, given a certain Γ coupling strength with the leads, G is a universal function of the rescaled coupling $\tilde{\lambda}$. This coupling represents the two competing energy/timescales of the nanowire-QD system: MZM lifetime τ_M and the inverse of the nanowire-QD coupling strength $\sim|\lambda_{nw-d}|^2$.

While the above expression is strictly only exact for this toy model, it agrees with the numerical results of Fig. 3 for the weak nanowire-dot coupling limit. The main features of the conductance curves can be seen by inspection of Eq. (15). For a perfect MZM with $\tau_M \to \infty$, $G_{\text{peak}} = e^2/h$ if the QD is decoupled from the MZM, while $G_{\text{peak}} = e^2/2h$ for any finite λ_{nw-d}. For a finite τ_M, $G_{\text{peak}} > e^2/2h$. Specifically, reducing τ_M would smoothly increase the peak conductance to e^2/h. Moreover, a larger λ_{nw-d} brings G_{peak} closer to the quantized value $e^2/2h$. However, as the nanowire-dot coupling strength increases, the toy model needs to be modified to include the Floquet structure of the Green's function. This is analyzed in the next section.

2. *Floquet Green's function correction*

Due to their time periodicity, FMZMs can be expanded as $\eta(t) = \sum_n e^{-in\Omega t}\,\eta_n$, and since their quasienergy $\epsilon = 0$, the Green's function is given by

$$Q^R_\eta(n,\omega) = \sum_{k=-\infty}^{\infty} \frac{\eta_{k+n}(\eta_k)^*}{\omega - k\Omega + i\Gamma_M(\omega)}, \tag{16}$$

where the $\Gamma_M(\omega)$ must be the same for each k due to the Floquet theorem, as shown in [65]. By definition, we have $\eta^\dagger(t) = \eta(t)$, and therefore $(\eta_n)^* = \eta_{-n}$. Hence, for $n = 0$ the Green's function can be written as

$$Q^R_\eta(0,\omega) = \frac{C_0}{\omega + i\Gamma_M(\omega)} + \sum_{k=1}^{\infty} \frac{2C_k[\omega + i\Gamma_M(\omega)]}{[\omega + i\Gamma_M(\omega)]^2 - (k\Omega)^2}, \tag{17}$$

where $C_k \equiv \eta_k(\eta_k)^*$, so that $C_k \geqslant 0$. These k-dependent factors can be considered as decaying as a function of k due to the properties of the Fourier series. For our numerical calculations we set $C_k \sim k^{-\alpha}$, $\alpha = 2$. Different choices for the form of the decaying C_k lead to qualitatively similar results.

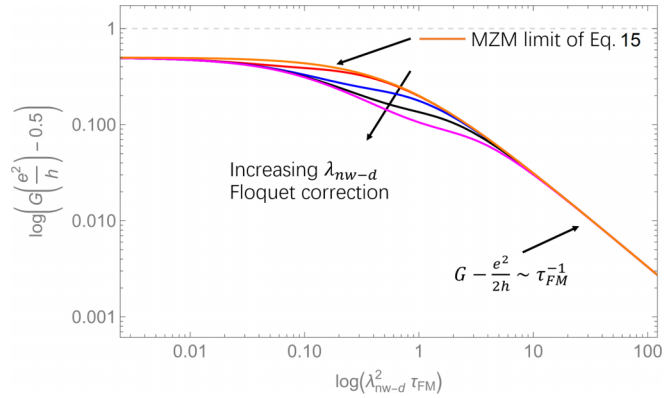

FIG. 4. Log-log plot of the conductance $G - e^2/2h$ from Eq. (19) using our toy model corrected for the Floquet structure of the FMZM Green's function, Eq. (16). In this plot, $C_k \sim k^{-\alpha}$, $\alpha = 2$. The figure shows that, with increasing λ_{nw-d}, the curve deviates from the low-λ_{nw-d} limit of Eq. (15), which is shown in orange, only for small enough lifetimes. The values set for λ_{nw-d} are 1.0 (red line, almost overlapping with the orange line), 2.0 (blue) and 3.0 (black), and 4.0 (magenta). The values are chosen arbitrarily in order to show the qualitative behavior due to the Floquet structure, with $\Omega = 12.0$.

The dot Green's function becomes

$$Q^R_{dd}(\omega) = \frac{\left[1 - \frac{|\lambda_{nw-d}|^2}{(\omega+2i\Gamma)}Q^R_\eta(0,\omega)\right]}{(\omega+2i\Gamma)\left[1 - \frac{2|\lambda_{nw-d}|^2}{(\omega+2i\Gamma)}Q^R_\eta(0,\omega)\right]}. \tag{18}$$

From this expression, the generalization of Eq. (15) is easily obtained as

$$G(\tilde{\lambda}) = \frac{e^2}{h}\frac{1 + |\tilde{\lambda}|^2/2\Gamma\left(A^0 + \sum_{k=1}^{\infty}\frac{2A^k\Gamma_M^2}{\Gamma_M^2+(k\Omega)^2}\right)}{1 + |\tilde{\lambda}|^2/\Gamma\left(A^0 + \sum_{k=1}^{\infty}\frac{2A^k\Gamma_M^2}{\Gamma_M^2+(k\Omega)^2}\right)}, \tag{19}$$

where $\Gamma_M \equiv \Gamma_M(\omega \to 0)$. Note that the introduction of the energy scale defined by $\hbar\Omega$ does not allow G to be a universal function of the dimensionless parameter $\tilde{\lambda}$, since the expression in brackets has a dependence on the FMZM width Γ_M. In the $\Omega \to \infty$ limit, the expression reduces to the previous model. We can also check the relevant limits of Eq. (19) in the same way that we did for Eq. (15). For the uncoupled dot, $G = e^2/h$, and the large-τ_{FM} limit, ($\Gamma_M \to 0$) leads to $G = e^2/2h$, with the Floquet contribution (second term in the bracket) vanishing. This leads to a $G(\tilde{\lambda})$ as reported in Fig. 4. The results show a deviation from the form of Eq. (15) for shorter lifetimes while maintaining the same $G - 1/2 \sim \tau_{FM}^{-1}$ behavior for long lifetimes, in agreement with our numerical results.

To summarize, in this section we showed that the conductance through a resonant quantum dot as a function of the rescaled coupling/lifetime $|\lambda_{nw-d}|^2\tau_{FM}$ has a characteristic functional form, which is almost identical when the dot is coupled to either dissipative MZMs or FMZMs, with the conductance curves differing only for short lifetimes and strong enough nanowire-dot coupling. In particular, given the possibility of tuning of the FMZMs' lifetime and the nanowire-dot coupling strength, our results provide a signature for the presence and stability—in terms of their lifetimes—of FMZMs in

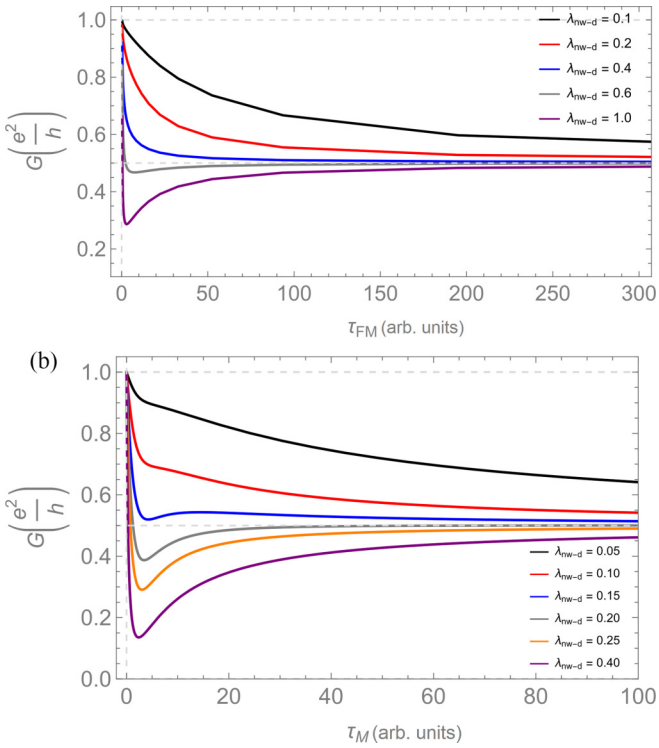

FIG. 5. (a) Same plot as Fig. 3, showing $G < e^2/2h$ for short τ_{FM} and large λ_{nw-d}, where the model parameters have been modified to get FMZMs with smaller $\Delta_{ind} = 0.64$. Specifically, $t_h = 1.0$ ($D = 4.0$), $\alpha = 1.5$, $V_z = V_z^d = 1.2$, $V = 0.8$, $\Omega = 6.0$, and $0 \leqslant A \leqslant 5.2$, as in Fig. 3, with a Floquet matrix cutoff $N_F = 20$. (b) $G(\tau_M)$ from Eq. (21) for the toy model with an additional off-resonant fermion. We can see that the model can qualitatively reproduce the large-λ short-lifetime behavior shown in (a). Equation (21) is computed with $\Gamma = 0.1$, $\delta = 0.3$.

topological nanowires. The QD conductance should behave as shown in Figs. 3 and 4 and as described by Eqs. (15) and (20).

In the next section we briefly explore how the QD conductance is modified if other modes in the nanowire also couple to the QD, which happens when $\lambda_{nw-dot} \gtrsim \Delta_{ind}$ through the influence of above-gap states. Moreover, we consider the case of the QD being off-resonance and finite-temperature corrections to G.

C. Soft SC gap (coupling to a normal fermion), nonresonant QD, and finite-temperature effects

A setting in which the undesired coupling could happen is the case in which the nanowire-dot coupling gets too large; the coupling of states above the induced gap can affect the value of the conductance. For instance, this effect can manifest itself when engineering very short FMZM lifetimes, corresponding to larger amplitudes in the drive, as explained in Sec. II B and as established in [65]. In such a case the spectrum in the nanowire is broadened and the SC gap derived from the Floquet GF becomes soft [64]. The effect on the conductance is shown in Fig. 5(a), where we modify our model parameters and we set some $\lambda_{nw-d} \gtrsim \Delta_{ind}$; the numerical results show values $G < e^2/2h$ when approaching shorter FMZM lifetimes. However, these conductance curves show a minimum for small τ_{FM}, reverting to $G \to e^2/h$ for $\tau_{FM} \to 0$. A value of $G = 0$ is a signature of a dot coupled to a normal fermion. Hence the features seen in the figure are probably due to the contribution of states above the induced gap, detected via the strong coupling. However, since such quasiparticles also acquire a finite lifetime due to the drive and dissipation, the limit $G(\tau \to 0) = e^2/h$ should be maintained.

To analyze this behavior, we add to the MZM a normal fermion with finite width $\Gamma_f(\omega)$ and with finite energy δ—slightly off-resonant with the QD—to the MZM toy model. Hence, the GF become, in particle-hole space,

$$Q^R_{nw}(\omega) \approx \begin{pmatrix} \frac{1}{\omega+i\Gamma_M} + \frac{1}{\omega-\delta+i\Gamma_f} & 0 \\ 0 & \frac{1}{\omega+i\Gamma_M} + \frac{1}{\omega+\delta+i\Gamma_f} \end{pmatrix}. \quad (20)$$

In order to derive the simplest possible expression for G capturing the numerics, we make the following assumptions: The lifetimes of both the MZM and the off-resonant fermion are set to be the same $\Gamma_f = \Gamma_M \equiv 1/\tau_M$, as well as the nanowire-QD coupling λ_{nw-d}. This leads to the following expression for the conductance ($\epsilon_d = 0$):

$$G(\tau_M) = \frac{e^2}{h} \frac{1 + \delta^2 |\lambda_{nw-d}|^2 \tau_M / [2\Gamma(\delta^2 + 1/\tau_M^2)]}{1 + |\lambda_{nw-d}|^2 \left[\frac{\tau_M}{\Gamma} + \frac{1}{\delta^2 + \frac{1}{\tau_M^2}} \left(\frac{1}{\Gamma\tau_M} + \frac{|\lambda_{nw-d}|^2}{2\Gamma^2}\right)\right]}. \quad (21)$$

A plot of the above function is shown in Fig. 5(b). The model is able to replicate the small-τ_M/large-λ features of the numerical simulation of 5(a), which we can now explain as follows. On the one hand, the FMZM lifetime is reduced by dissipation, leading to a reduced "effective coupling" $\tilde{\lambda}$ to the dot. On the other hand, the effect of SC gap softening in the nanowire as the amplitude of the periodic drive is increased can lead to a signal $G \to 0$ as the dot starts coupling to a normal fermion above the gap. This effect only becomes important as the nanowire-QD coupling $\lambda_{nw-dot} \gtrsim \Delta_{ind}$. An assumption that was made so far is that of a resonant dot. If the QD energy level $\epsilon_d \neq 0$, then the $G(\tau_{FM} \to 0) < e^2/h$, with the expression for the conductance of Eq. (15) becoming

$$G(\tilde{\lambda}) = \frac{e^2}{h} \frac{1 + C_0 |\tilde{\lambda}|^2 / 2\Gamma}{1 + C_0 |\tilde{\lambda}|^2 / \Gamma + (\epsilon_d / 2\Gamma)^2}, \quad (22)$$

which agrees with our numerical results when we choose $\epsilon_d \neq 0$ for weak nanowire-QD coupling, as shown in Fig. 6—Eq. (19) for the Floquet case is similarly modified by adding the $(\epsilon_d/2\Gamma)^2$ term in the denominator, showing the same qualitative behavior as the above. The finite ϵ_d correction especially affects the small-τ_{FM} behavior, as clearly seen from Eq. (22). While it is in principle always possible to tune the QD to be resonant by measuring its conductance when uncoupled from the nanowire, it may not be straightforward in realistic experimental scenarios.

At finite temperature T, Fig. 6(c) shows that the value of the conductance changes with increasing T for longer FMZM lifetimes, an effect that is suppressed for a larger value for λ_{nw-d}, as long as the thermal energy scale is small enough compared to other energy scales. These effects need to be taken into account when considering the application of the conductance-lifetime relation of Eq. (15) to experimentally measure the FMZM lifetime.

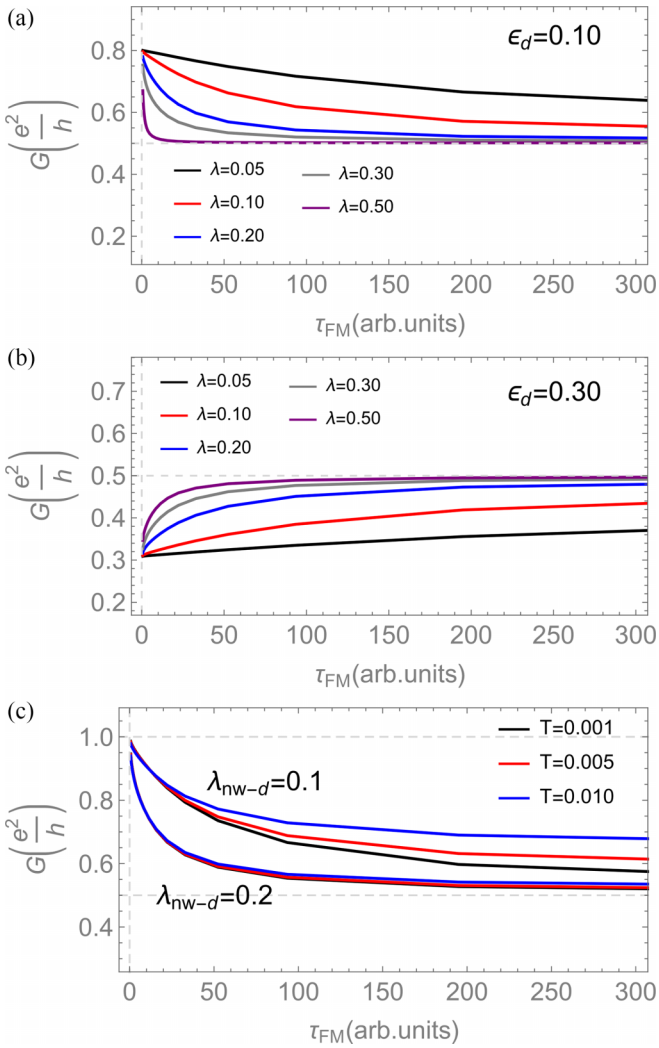

FIG. 6. Conductance $G(\tau_{FM})$ from Eq. (11) (arbitrary units), same parameters as in Fig. 3, QD energy level (a) $\epsilon_d = 0.1$ and (b) $\epsilon_d = 0.3$. We can see how, especially for short lifetimes, the values of the peak conductance get affected, with $G(\tau_{FM} \to 0) < e^2/h$ as described by Eq. (22). For three values of temperature T, (c) shows the conductance as computed from Eq. (9) with the same parameters as in Fig. 3, with a resonant QD and $\lambda_{nw-d} = 0.1,\ 0.2$. Note that the effect of temperature becomes negligible for large enough λ_{nw-d} compared to T.

IV. CONCLUSIONS

In this work we studied the transport signatures of dissipative FMZMs coupled to a resonant quantum dot. We derived an expression for the conductance from first principles via the Floquet-Keldysh formalism, allowing for a nonperturbative treatment. We showed that the peak conductance of a dot coupled to a FMZM shows a characteristic transition from the Majorana signature $G = e^2/2h$ to the uncoupled value $G = e^2/h$ as the FMZM lifetime decays. We showed that the peak conductance can be well approximated by a universal function of the FMZM lifetime, rescaled with respect to the nanowire-dot coupling strength, despite the fact that the true functional form of the conductance is in fact more complex due to the Floquet structure of the FMZM's GF. Indeed, we showed that the Floquet correction only becomes important at short lifetimes and strong nanowire-dot coupling.

Periodically driven nanowires seem to be a convenient platform for the study of the lifetime and stability of FMZMs, given the simple nanowire-QD coupling setup and tunability of the periodic drive. However, the setup requires a good degree of control and fine-tuning of the coupling strength with the QD, as well as making sure that the induced superconducting gap stays large enough under a strong periodic drive, which might represent obstacles for an experimental realization. In addition, our calculations showed that imperfections in QD energy level tuning and finite-temperature effects can affect the measured QD conductance in relation to the FMZM lifetime.

Nonetheless, with the above premises, our work illustrates a clear signature for the presence of FMZMs in topological nanowires, even when taking into account the effects of dissipation from the SC bath. In future work it would be interesting to include more realistic effects in the setup, such as disorder and imperfections in the periodically driven-dissipative nanowire, to study their effects on electronic transport.

ACKNOWLEDGMENTS

We thank Gu Zhang, Zhesen Yang, and Qinghong Yang for helpful discussions. This work was supported by the National Natural Science Foundation of China (Grants No. 11974198 and No. 12004040), Beijing Academy of Quantum Information Sciences, Beijing 100193, Innovation Program for Quantum Science and Technology (Grant No. 2021ZD0302400).

APPENDIX

1. Nanowire model and recursion method

After integrating out the bath degrees of freedom, the on-site retarded component of the nanowire Floquet Green's function (GF) takes the form

$$\underline{g_i(\omega)} = [\underline{\omega} - \underline{H_{\text{eff},i}(\omega)}]^{-1}, \tag{A1}$$

where the on-site effective Floquet Hamiltonian is

$$\underline{H_{\text{eff},i}(\omega)} = \begin{pmatrix} \ddots & & & \\ & H_{nw,i} - \Omega + \Sigma_{sc}(\omega+\Omega) & A\sigma_0\tau_z & 0 \\ & A\sigma_0\tau_z & H_{nw,i} + \Sigma_{sc}(\omega) & A\sigma_0\tau_z \\ & 0 & A\sigma_0\tau_z & H_{nw,i} + \Omega + \Sigma_{sc}(\omega-\Omega) \\ & & & \ddots \end{pmatrix}, \tag{A2}$$

where $H_{nw,i} = (2t_h - \mu)\sigma_0\tau_z + V_z\sigma_z\tau_z$ and the bath self-energy term is [65]

$$\Sigma_{sc}(\omega) = V^2 \frac{1}{\sqrt{-(\omega + i\eta)^2 + \Delta^2}}[-(\omega + i\eta) - \Delta\sigma_y\tau_y], \tag{A3}$$

where $\eta = 0^+$ and the bath DOS is assumed to be uniform. For the numerical calculations η is set to a finite positive value, much smaller than any other energy scale in the system. The notation $\underline{M}$ indicates a matrix in Floquet space, which is in principle infinite-dimensional due to the Fourier expansion, and we denote this by $[\underline{M}]_{mn}$.

For instance, in Eq. (A2) $[\underline{H_{\text{eff},i}(\omega)}]_{nn} = H_{nw,i} + \Sigma_{sc}(\omega - n\Omega) + n\Omega$. In $\underline{H_{\text{eff},i}(\omega)}$ the off-diagonal elements represent the harmonic drive. A value of $\kappa \equiv A/\Omega < 1$ ensures convergence and allows for the truncation of the matrices in the Floquet Hilbert space for any value of Ω, and the matrix dimensions can be kept conveniently small without any appreciable loss of accuracy [65,66]. Moreover, the $Q(0,\omega)$ elements of the Floquet GF used in the main text to compute time averages of observables are extracted from the $[\underline{Q_{dd}(\omega)}]_{00}$ component of the Floquet GF matrix. The meaning of the self-energy of Eq. (A3) is that it represents dissipation through its ω dependence, i.e., a broadening of the quasiparticle spectrum via its imaginary part; when $\Delta < \Omega$, the self-energy of $[\underline{H_{\text{eff},i}(\omega)}]_{11/-1-1}$ becomes purely imaginary, which means that "single-photon" Floquet transitions lead to energy-particle exchange directly above the SC bath; when $\Delta > \Omega$, higher-order transitions are necessary and therefore the FMZM lifetime is longer. The nondissipative limit is found by letting $\Delta \to \infty$, whence $\Sigma_{sc} = \Delta_{ind}\sigma_y\tau_y$, with the self-energy simply becoming a real-valued induced gap parameter in the nanowire, with $\Delta_{ind} \equiv \rho_F V^2$.

The spectrum and local density of states of the FMZMs at the end of the nanowire can be calculated from the retarded part of the local GF, which is found by using the following recursive matrix equation in the Floquet-Keldysh-BdG space [65],

$$\underline{Q_{i+1,i+1}}(\omega) = \left[\underline{g_i}^{-1}(\omega) - \underline{T_{i+1,i}}\underline{Q_{i,i}}(\omega)\underline{T_{i,i+1}}\right]^{-1}, \tag{A4}$$

where $\underline{g_i}(\omega)$ is the on-site "bare" GF defined in Eq. (A1). The above equation is iterated for $N = 200$ sites in our calculations, with an appropriate N_F Floquet matrix cutoff to ensure convergence. The hopping matrix in the nanowire is

$$T_{i,i+1} = {T_{i+1,i}}^T = \begin{pmatrix} -t_h & 0 & -\alpha/2a & 0 \\ 0 & t_h & 0 & \alpha/2a \\ \alpha/2a & 0 & -t_h & 0 \\ 0 & -\alpha/2a & 0 & t_h \end{pmatrix}, \tag{A5}$$

which, extended in F-K-BdG space, is simply $\underline{T_{i,i+1}} = I_{2N_F+1} \otimes I_2 \otimes T_{i,i+1}$.

The quantum dot coupled to the leads of Eq. (5) can be included as an additional site of the recursive chain, which means that we need to perform an additional iteration of Eq. (A4) with $g^{-1}(\omega) = \text{diag}[\omega - \epsilon_d - V_z^d + i(\Gamma_L + \Gamma_R), \omega - \epsilon_d + V_z^d + i(\Gamma_L + \Gamma_R), \omega + \epsilon_d + V_z^d + i(\Gamma_L + \Gamma_R), \omega + \epsilon_d - V_z^d + i(\Gamma_L + \Gamma_R)]$ and $T_{i,i+1} = \text{diag}[-\lambda_{nw-d}, \lambda_{nw-d}, -\lambda_{nw-d}, \lambda_{nw-d}]$.

2. Derivation of the current and conductance using Floquet-Keldysh field theory

In order to derive the expression of conductance of Eq. (9) in the main text, one can start from the effective action with current source term [76]

$$S = S_0 + S_{L-D} + S_{\text{source}}, \tag{A6}$$

where

$$S_0 = \sum_{kk',\alpha=L,R} \int_C \int_C dt dt' \Psi^\dagger_{k,\alpha}(t) Q^{-1}_{0,kk'\alpha}(t,t') \Psi_{k',\alpha}(t') + \int_C \int_C dt dt' \Psi^\dagger_d(t) Q^{-1}_{0,dd}(t,t') \Psi_d(t'), \tag{A7}$$

and the coupling part of the action is given by

$$S_{L-D} = \sum_{k\alpha} \int_C dt (\lambda_{k\alpha} c^\dagger_{k\alpha} d + \text{H.c.}) = \sum_{k\alpha} \int_C dt (\Psi^\dagger_{k,\alpha}(t) \hat{M}_{T,k\alpha} \Psi_d(t) + \text{H.c.}), \tag{A8}$$

where we choose to work in the Nambu basis $\Psi^\dagger_{k,\alpha} = (c^\dagger_{k,\alpha}, c_{k,\alpha})/\sqrt{2}$ and $\Psi^\dagger_d = (d^\dagger, d)/\sqrt{2}$; the tunneling matrix element is $M_{T,k\alpha} = \left(\begin{smallmatrix} \lambda_{\alpha k} & 0 \\ 0 & -\lambda^*_{\alpha k} \end{smallmatrix}\right)$; $Q_{0,dd}(t,t')$ is the Green's operator for the dot; and $Q_{0,kk'\alpha}(t,t')$ is the Green's function of the lead.

By defining a spinor for the whole space $\Psi^\dagger = (l^\dagger_{kL}, l_{kL}, d^\dagger, d, l^\dagger_{kR}, l_{kR})/\sqrt{2}$, the above action terms can be expressed as

$$S_0 + S_{L-D} = \int_C \int_C dt dt' \Psi^\dagger(t) Q^{-1}(t,t') \Psi(t'), \tag{A9}$$

where the Green's function is

$$Q_{kk'} = \begin{pmatrix} Q_{Lk,Lk'} & Q_{Lk,d} & Q_{Lk,Rk'} \\ Q_{d,Lk'} & Q_{d,d} & Q_{d,Rk'} \\ Q_{Rk,Lk'} & Q_{Rk,d} & Q_{Rk,Rk'} \end{pmatrix}. \tag{A10}$$

Out of these components, for the transport calculations we only need the Q_{dd} from the dot, as we will show in the following derivation.

Finally, the source term is defined as

$$S_{\text{source}} = -\int dt A(t) I_L(t) = -\sum_{a,b=1}^{2} \int_{-\infty}^{\infty} dt \bar{\Psi}_a \hat{A}_{ab} \hat{M}_L \Psi_b, \tag{A11}$$

where the spinors and matrices are now in Keldysh space after performing a Larkin-Ovchinnikov rotation, where $\hat{A} = A^q \gamma^q$, $\gamma^q = \sigma_1$, and the Keldysh spinors $\Psi_{1,2}$, $\bar{\Psi}_{1,2}$ are defined as $\Psi_{1/2} = (\Psi^+ \pm \Psi^-)/\sqrt{2}$ and $\bar{\Psi}_{1/2} = (\bar{\Psi}^+ \mp \bar{\Psi}^-)/\sqrt{2}$, where Ψ^+ and Ψ^- are the components of the Grassmann field Ψ that reside on the forward and backward parts of the time contour C, respectively [77]. The retarded, advanced, and Keldysh components of the Green's function are defined as

(with $a, b \in \{1, 2\}$) [77,78]

$$Q_{ab}(t,t') = -i\,\langle \Psi_a(t)\bar{\Psi}_b(t')\rangle = \begin{pmatrix} Q^R(t,t') & Q^K(t,t') \\ 0 & Q^A(t,t') \end{pmatrix}, \tag{A12}$$

where the retarded, advanced, and Keldysh components have the usual definitions $Q^{R/A}(t,t') = \mp i\theta(\pm t \mp t')\langle\{\Psi(t), \Psi^\dagger(t')\}\rangle$ and $Q^K = -i(\langle\Psi^-(t)\bar{\Psi}^+(t')+\rangle\langle\Psi^+(t)\bar{\Psi}^-(t')\rangle)$.

The source term of Eq. (A11) generates the current through the left lead

$$I_L(t) = \frac{ie}{\hbar}\sum_{k\sigma}(\lambda_{Lk} l^\dagger_{Lk\sigma} d_\sigma - \lambda^*_{Lk\sigma} d^\dagger_\sigma l_{Lk\sigma}) = \vec{\Psi}^\dagger(t)\hat{M}_L\vec{\Psi}(t). \tag{A13}$$

The transport matrix $\hat{M}_L$ is defined as

$$\hat{M}_L = \frac{ie}{\hbar}\begin{pmatrix} 0 & M_L^{12} & 0 \\ M_L^{21} & 0 & 0 \\ 0 & 0 & 0 \end{pmatrix}, \tag{A14}$$

with $M_L^{12} = \left(\begin{smallmatrix}\lambda_{Lk} & 0 \\ 0 & \lambda^*_{Lk}\end{smallmatrix}\right)$ and $M_L^{21} = \left(\begin{smallmatrix}-\lambda^*_{Lk} & 0 \\ 0 & -\lambda_{Lk}\end{smallmatrix}\right)$. The generating function is $Z[A] = \int D[\bar{\Psi}\Psi]e^{iS}$, and upon Gaussian integration to linear order in A^q, $\ln Z[A] = \mathrm{Tr}\ln[\hat{1} - QAM] \approx -\mathrm{Tr}[QA^q\gamma^q M_L]$. The current can be expressed as

$$I_L(t) = \frac{i}{2}\frac{\delta \ln Z[A]}{\delta A^q}\bigg|_{A^q=0} \approx -\frac{i}{2}\mathrm{Tr}[Q(t,t)\gamma^q M_L], \tag{A15}$$

leading to

$$I_L(t) = \frac{e}{2\hbar}\sum_k\sum_n\int\frac{d\omega}{2\pi}e^{in\Omega t}\mathrm{Tr}\big[Q^K_{Lk,d}(n,\omega)M_L^{21} + Q^K_{d,Lk}(n,\omega)M_L^{12}\big], \tag{A16}$$

where the trace over the lead-QD space has been performed, and the following identity was applied:

$$\mathrm{Tr}[Q_\alpha\gamma^q] = Q^K_\alpha(t,t) = \sum_n\int\frac{d\omega}{2\pi}e^{in\Omega t}Q^K(n,\omega), \tag{A17}$$

where Q^K is the Keldysh component of the Green's function. The above Green's functions (for the left lead) can be expressed as follows, in terms of the lead GF g^0_{Lk} and dot GF Q_{dd}:

$$Q_{d,Lk} = M_T^{21}Q_{dd}g^0_{Lk}, \tag{A18}$$

$$Q_{Lk,d} = M_T^{12}g^0_{Lk}Q_{dd}. \tag{A19}$$

Taking the Keldysh component of these products leads to

$$(Q_{d,Lk})^K = M_T^{21}\big[(Q_{dd})^R\big(g^0_{Lk}\big)^K + (Q_{dd})^K\big(g^0_{Lk}\big)^A\big], \tag{A20}$$

and

$$(Q_{Lk,d})^K = M_T^{12}\big[\big(g^0_{Lk}\big)^R(Q_{dd})^K + \big(g^0_{Lk}\big)^K(Q_{dd})^A\big], \tag{A21}$$

where $(Q, g^0)^{R/A}$ are the QD/lead Green's function retarded and advanced components. Upon substitution in Eq. (A16), it leads to the following expression for the time-dependent current:

$$I_L(t) = \frac{ie}{2\hbar}\sum_n e^{in\Omega t}\int\frac{d\omega}{2\pi}\Gamma_L\{[1-2n_L(\omega)] \times \big[{Q_{dd}}^R(n,\omega) - {Q_{dd}}^A(n,\omega)\big] - {Q_{dd}}^K(n,\omega)\}, \tag{A22}$$

where $n_L(\omega)$ is the Fermi-Dirac distribution of the L lead. Note that at this stage the expression shows the exact current with its full time dependence. The only assumption, as stated in the main text, is that the system is in a nonequilibrium steady state, and thus the Green's function is periodic in time with the period τ of the drive. In addition, for the derivation of Eq. (A22), the following are used:

(1) Identities for the lead GF, $[g^0_{Lk}(\omega)]^K = -2\pi i\delta(\omega - \epsilon_k)[1-2n_L(\omega)]$ and $[g^0_{Lk}(\omega)]^R - [g^0_{Lk}(\omega)]^A = -2\pi i\delta(\omega - \epsilon_k)$.

(2) The summation over k is performed with the help of the δ function, and we assume the wide-band limit for the leads, with a constant density of states $\rho(\omega) = \rho_{Fl}$.

(3) The linewidth function is defined as $\Gamma_L = 2\pi\rho_{Fl}|\lambda_L|^2$.

The equivalent expression can also be derived for $I_R(t)$, defined as

$$I_R(t) = \frac{ie}{\hbar}\sum_{k\sigma}(\lambda_{Rk} l^\dagger_{Rk\sigma} d_\sigma - \lambda^*_{Rk\sigma} d^\dagger_\sigma l_{Rk\sigma}). \tag{A23}$$

For a time-dependent system, $I_L(t) = -I_R(t)$ only holds for time averages, i.e., $\langle I_L(t)\rangle = -\langle I_R(t)\rangle$ [79].

Therefore for the time-averaged current through the dot $\langle I\rangle = \langle(I_L - I_R)/2\rangle$, the following simple expression for the current is valid:

$$\langle I\rangle = \frac{ie}{\hbar}\int\frac{d\omega}{2\pi}[n_F^L(\omega) - n_F^R(\omega)] \times\mathrm{Tr}\left\{\frac{\Gamma_L\Gamma_R}{\Gamma_L+\Gamma_R}[Q^R_{dd}(0,\omega) - Q^A_{dd}(0,\omega)]\right\}. \tag{A24}$$

This leads directly to the expression for the conductance of Eq. (9) in the main text.

[1] N. Read and D. Green, Phys. Rev. B **61**, 10267 (2000).
[2] A. Y. Kitaev, Phys. Usp. **44**, 131 (2001).
[3] A. Y. Kitaev, Ann. Phys. **303**, 2 (2003).
[4] C. Nayak, S. H. Simon, A. Stern, M. Freedman, and S. Das Sarma, Rev. Mod. Phys. **80**, 1083 (2008).
[5] J. M. Leinaas and J. Myrheim, Il Nuovo Cimento B (1971-1996) **37**, 1 (1977).
[6] K. Fredenhagen, K.-H. Rehren, and B. Schroer, Commun. Math. Phys. **125**, 201 (1989).
[7] D. A. Ivanov, Phys. Rev. Lett. **86**, 268 (2001).
[8] J. D. Sau, R. M. Lutchyn, S. Tewari, and S. Das Sarma, Phys. Rev. Lett. **104**, 040502 (2010).
[9] R. M. Lutchyn, J. D. Sau, and S. Das Sarma, Phys. Rev. Lett. **105**, 077001 (2010).

[10] Y. Oreg, G. Refael, and F. von Oppen, Phys. Rev. Lett. **105**, 177002 (2010).
[11] J. Alicea, Phys. Rev. B **81**, 125318 (2010).
[12] J. Alicea, Rep. Prog. Phys. **75**, 076501 (2012).
[13] V. Mourik, K. Zuo, S. M. Frolov, S. Plissard, E. P. Bakkers, and L. P. Kouwenhoven, Science **336**, 1003 (2012).
[14] M. Deng, C. Yu, G. Huang, M. Larsson, P. Caroff, and H. Xu, Nano Lett. **12**, 6414 (2012).
[15] A. Das, Y. Ronen, Y. Most, Y. Oreg, M. Heiblum, and H. Shtrikman, Nat. Phys. **8**, 887 (2012).
[16] H. O. H. Churchill, V. Fatemi, K. Grove-Rasmussen, M. T. Deng, P. Caroff, H. Q. Xu, and C. M. Marcus, Phys. Rev. B **87**, 241401(R) (2013).
[17] A. D. K. Finck, D. J. Van Harlingen, P. K. Mohseni, K. Jung, and X. Li, Phys. Rev. Lett. **110**, 126406 (2013).
[18] S. M. Albrecht, A. P. Higginbotham, M. Madsen, F. Kuemmeth, T. S. Jespersen, J. Nygård, P. Krogstrup, and C. Marcus, Nature (London) **531**, 206 (2016).
[19] M. Deng, S. Vaitiekėnas, E. B. Hansen, J. Danon, M. Leijnse, K. Flensberg, J. Nygård, P. Krogstrup, and C. M. Marcus, Science **354**, 1557 (2016).
[20] H. Zhang, Ö. Gül, S. Conesa-Boj, M. P. Nowak, M. Wimmer, K. Zuo, V. Mourik, F. K. De Vries, J. Van Veen, M. W. De Moor *et al.*, Nat. Commun. **8**, 16025 (2017).
[21] Ö. Gül, H. Zhang, J. D. Bommer, M. W. de Moor, D. Car, S. R. Plissard, E. P. Bakkers, A. Geresdi, K. Watanabe, T. Taniguchi *et al.*, Nat. Nanotechnol. **13**, 192 (2018).
[22] H. Zhang, M. W. de Moor, J. D. Bommer, D. Xu, G. Wang, N. van Loo, C.-X. Liu, S. Gazibegovic, J. A. Logan, D. Car *et al.*, arXiv:2101.11456.
[23] Z. Wang, H. Song, D. Pan, Z. Zhang, W. Miao, R. Li, Z. Cao, G. Zhang, L. Liu, L. Wen, R. Zhuo, D. E. Liu, K. He, R. Shang, J. Zhao, and H. Zhang, Phys. Rev. Lett. **129**, 167702 (2022).
[24] Z. Wang, S. Zhang, D. Pan, G. Zhang, Z. Xia, Z. Li, D. Liu, Z. Cao, L. Liu, L. Wen, D. Liao, R. Zhuo, Y. Li, D. E. Liu, R. Shang, J. Zhao, and H. Zhang, Phys. Rev. B **106**, 205421 (2022).
[25] H. Song, Z. Zhang, D. Pan, D. Liu, Z. Wang, Z. Cao, L. Liu, L. Wen, D. Liao, R. Zhuo, D. E. Liu, R. Shang, J. Zhao, and H. Zhang, Phys. Rev. Res. **4**, 033235 (2022).
[26] M. Aghaee, A. Akkala, Z. Alam, R. Ali, A. A. Ramirez, M. Andrzejczuk, A. E. Antipov, M. Astafev, B. Bauer, J. Becker *et al.*, arXiv:2207.02472.
[27] A. Eckardt, Rev. Mod. Phys. **89**, 011004 (2017).
[28] T. Oka and S. Kitamura, Annu. Rev. Condens. Matter Phys. **10**, 387 (2019).
[29] M. S. Rudner and N. H. Lindner, Nat. Rev. Phys. **2**, 229 (2020).
[30] A. Castro, U. De Giovannini, S. A. Sato, H. Hübener, and A. Rubio, Phys. Rev. Res. **4**, 033213 (2022).
[31] N. H. Lindner, G. Refael, and V. Galitski, Nat. Phys. **7**, 490 (2011).
[32] T. Kitagawa, T. Oka, A. Brataas, L. Fu, and E. Demler, Phys. Rev. B **84**, 235108 (2011).
[33] J. P. Dahlhaus, J. M. Edge, J. Tworzydło, and C. W. J. Beenakker, Phys. Rev. B **84**, 115133 (2011).
[34] L. Jiang, T. Kitagawa, J. Alicea, A. R. Akhmerov, D. Pekker, G. Refael, J. I. Cirac, E. Demler, M. D. Lukin, and P. Zoller, Phys. Rev. Lett. **106**, 220402 (2011).
[35] T. Kitagawa, M. A. Broome, A. Fedrizzi, M. S. Rudner, E. Berg, I. Kassal, A. Aspuru-Guzik, E. Demler, and A. G. White, Nat. Commun. **3**, 882 (2012).
[36] A. A. Reynoso and D. Frustaglia, Phys. Rev. B **87**, 115420 (2013).
[37] D. E. Liu, A. Levchenko, and H. U. Baranger, Phys. Rev. Lett. **111**, 047002 (2013).
[38] T. Iadecola, D. Campbell, C. Chamon, C.-Y. Hou, R. Jackiw, S.-Y. Pi, and S. V. Kusminskiy, Phys. Rev. Lett. **110**, 176603 (2013).
[39] B. M. Fregoso, Y. H. Wang, N. Gedik, and V. Galitski, Phys. Rev. B **88**, 155129 (2013).
[40] T. Iadecola, T. Neupert, and C. Chamon, Phys. Rev. B **89**, 115425 (2014).
[41] L. E. F. Foa Torres, P. M. Perez-Piskunow, C. A. Balseiro, and G. Usaj, Phys. Rev. Lett. **113**, 266801 (2014).
[42] T. A. Sedrakyan, V. M. Galitski, and A. Kamenev, Phys. Rev. Lett. **115**, 195301 (2015).
[43] M. C. Rechtsman, J. M. Zeuner, Y. Plotnik, Y. Lumer, D. Podolsky, F. Dreisow, S. Nolte, M. Segev, and A. Szameit, Nature (London) **496**, 196 (2013).
[44] A. C. Potter, T. Morimoto, and A. Vishwanath, Phys. Rev. X **6**, 041001 (2016).
[45] R. Roy and F. Harper, Phys. Rev. B **96**, 155118 (2017).
[46] R. W. Bomantara and J. Gong, Phys. Rev. Lett. **120**, 230405 (2018).
[47] R. W. Bomantara and J. Gong, Phys. Rev. B **98**, 165421 (2018).
[48] Y. Peng and G. Refael, Phys. Rev. B **98**, 220509(R) (2018).
[49] Y. H. Wang, H. Steinberg, P. Jarillo-Herrero, and N. Gedik, Science **342**, 453 (2013).
[50] F. Mahmood, C.-K. Chan, Z. Alpichshev, D. Gardner, Y. Lee, P. A. Lee, and N. Gedik, Nat. Phys. **12**, 306 (2016).
[51] S. Aeschlimann, S. A. Sato, R. Krause, M. Chávez-Cervantes, U. De Giovannini, H. Hübener, S. Forti, C. Coletti, K. Hanff, K. Rossnagel, A. Rubio, and I. Gierz, Nano Letters, Nano Lett. **21**, 5028 (2021).
[52] T. Mori, T. Kuwahara, and K. Saito, Phys. Rev. Lett. **116**, 120401 (2016).
[53] D. A. Abanin, W. De Roeck, W. W. Ho, and F. Huveneers, Phys. Rev. B **95**, 014112 (2017).
[54] D. Abanin, W. De Roeck, W. W. Ho, and F. Huveneers, Commun. Math. Phys. **354**, 809 (2017).
[55] P. Ponte, A. Chandran, Z. Papić, and D. A. Abanin, Ann. Phys. **353**, 196 (2015).
[56] C. W. von Keyserlingk and S. L. Sondhi, Phys. Rev. B **93**, 245145 (2016).
[57] J. Zhang, P. W. Hess, A. Kyprianidis, P. Becker, A. Lee, J. Smith, G. Pagano, I.-D. Potirniche, A. C. Potter, A. Vishwanath *et al.*, Nature (London) **543**, 217 (2017).
[58] S. Choi, J. Choi, R. Landig, G. Kucsko, H. Zhou, J. Isoya, F. Jelezko, S. Onoda, H. Sumiya, V. Khemani *et al.*, Nature (London) **543**, 221 (2017).
[59] B. Bauer, T. Pereg-Barnea, T. Karzig, M.-T. Rieder, G. Refael, E. Berg, and Y. Oreg, Phys. Rev. B **100**, 041102(R) (2019).
[60] D. W. Hone, R. Ketzmerick, and W. Kohn, Phys. Rev. E **79**, 051129 (2009).
[61] T. Iadecola, T. Neupert, and C. Chamon, Phys. Rev. B **91**, 235133 (2015).
[62] D. E. Liu, Phys. Rev. B **91**, 144301 (2015).

[63] K. I. Seetharam, C.-E. Bardyn, N. H. Lindner, M. S. Rudner, and G. Refael, Phys. Rev. X **5**, 041050 (2015).
[64] Q. Yang, Z. Yang, and D. E. Liu, Phys. Rev. B **104**, 014512 (2021).
[65] Z. Yang, Q. Yang, J. Hu, and D. E. Liu, Phys. Rev. Lett. **126**, 086801 (2021).
[66] D. E. Liu, A. Levchenko, and R. M. Lutchyn, Phys. Rev. B **95**, 115303 (2017).
[67] D. E. Liu and H. U. Baranger, Phys. Rev. B **84**, 201308(R) (2011).
[68] D. Liu, Z. Cao, X. Liu, H. Zhang, and D. E. Liu, Phys. Rev. B **104**, 205125 (2021).
[69] G. Kells, D. Meidan, and P. W. Brouwer, Phys. Rev. B **86**, 100503(R) (2012).
[70] C. Moore, T. D. Stanescu, and S. Tewari, Phys. Rev. B **97**, 165302 (2018).
[71] C. Moore, C. Zeng, T. D. Stanescu, and S. Tewari, Phys. Rev. B **98**, 155314 (2018).
[72] A. Vuik, B. Nijholt, A. R. Akhmerov, and M. Wimmer, SciPost Phys. **7**, 061 (2019).
[73] H. Pan and S. Das Sarma, Phys. Rev. Res. **2**, 013377 (2020).
[74] M. Grifoni and P. Hänggi, Phys. Rep. **304**, 229 (1998).
[75] O. Shtanko and R. Movassagh, Phys. Rev. Lett. **125**, 086804 (2020).
[76] D. E. Liu, M. Cheng, and R. M. Lutchyn, Phys. Rev. B **91**, 081405(R) (2015).
[77] A. Kamenev, *Field Theory of Non-Equilibrium Systems* (Cambridge University Press, Cambridge, England, 2011).
[78] A. Altland and B. D. Simons, *Condensed Matter Field Theory*, 2nd ed. (Cambridge University Press, England, 2010).
[79] H. Haug and A.-P. Jauho, *Quantum Kinetics in Transport and Optics of Semiconductors* (Springer, New York, 2008), Vol. 2.